FEBS Letters 588 (2014) 1886–1890

journal homepage: www.FEBSLetters.org

The X-ray crystal structure of *Shewanella oneidensis* OmcA reveals new insight at the microbe–mineral interface

Marcus J. Edwards [a], Nanakow A. Baiden [a], Alexander Johs [b], Stephen J. Tomanicek [b], Liyuan Liang [b], Liang Shi [c], Jim K. Fredrickson [c], John M. Zachara [c], Andrew J. Gates [a], Julea N. Butt [a], David J. Richardson [a,*], Thomas A. Clarke [a,*]

[a] *Centre for Molecular and Structural Biochemistry, School of Biological Sciences and School of Chemistry, University of East Anglia, Norwich NR4 7TJ, United Kingdom*
[b] *Environmental Sciences Division, Oak Ridge National Laboratory, Oak Ridge, TN 37831, USA*
[c] *Pacific Northwest National Laboratory, Richland, WA 99352, USA*

ARTICLE INFO

Article history:
Received 10 March 2014
Revised 3 April 2014
Accepted 4 April 2014
Available online 18 April 2014

Edited by Richard Cogdell

Keywords:
Multiheme cytochrome
Mineral respiration
Electron transfer
Shewanella
c-Type heme
Outer membrane
Metalloprotein

ABSTRACT

The X-ray crystal structure of *Shewanella oneidensis* OmcA, an extracellular decaheme cytochrome involved in mineral reduction, was solved to a resolution of 2.7 Å. The four OmcA molecules in the asymmetric unit are arranged so the minimum distance between heme 5 on adjacent OmcA monomers is 9 Å, indicative of a transient OmcA dimer capable of intermolecular electron transfer. A previously identified hematite binding motif was identified near heme 10, forming a hydroxylated surface that would bring a heme 10 electron egress site to ~10 Å of a mineral surface.

Structured summary of protein interactions:
OmcA and **OmcA** bind by X-ray crystallography (View interaction)

1. Introduction

Many species of Gram-negative bacteria can couple anaerobic growth to the respiratory reduction of extracellular insoluble minerals containing Fe(III) and Mn(III/IV), with which they can physically interact. Metal-reducing species within the genus *Shewanella* transfer electrons across the outer-membrane via a 'porin-cytochrome' electron transport module to extracellular deca- or undeca-heme cytochromes that serve either as direct reductases of multi-valent metals associated with minerals or as reductases of soluble metal chelates or electron shuttles, such as flavins [1]. The *Shewanella* family of outer membrane multi-heme cytochromes (OMMCs) form four major clades: the OmcA, MtrC, UndA and MtrF clades (Fig. S1). The molecular structure of two prototypical members of two clades have recently been resolved, the deca-heme MtrF of *Shewanella oneidensis* [2] and the undeca-heme *S. HRCR-6* UndA [3]. However, functional and biochemical data on these two OMMCs is limited. Of the *Shewanella* OMMCs, MtrC and OmcA have been the most widely studied [4–7]. They are exported to the extracellular environment by the type II secretion system [8] and Δ*omcA*–Δ*mtrC* double mutants are severely compromised for respiratory mineral Fe(III) reduction and electron transfer to anodes in microbial fuel cells [9]. Protein film voltammetry measurements have shown that *S. oneidensis* OmcA and MtrC can transfer electrons directly to graphite electrodes with interfacial ET rates that lie in range of ~100 to 300 s^{-1} [10,11]. A combination of methodologies, including fluorescence correlation spectroscopy, optical waveguide light-mode spectroscopy and protein film voltammetry (PFV), have also shown that *S. oneidensis* OmcA can bind and transfer electrons to hematite and ferrihydrite [12–15]. Neutron reflectometry showed that OmcA forms a well-defined monomolecular layer on hematite surfaces, where it assumes an orientation that maximizes its contact area with the mineral surface [16]. Given the wealth of biochemical and biophysical information on *S. oneidensis* OmcA, and clear demonstration of its capacity for direct electron transfer to Fe(III) minerals, it is critical to elucidate the underlying molecular architecture to gain a molecular-level understanding of the electron transfer processes

* Corresponding authors. Fax: +44 1603 592250.
E-mail addresses: d.richardson@uea.ac.uk (D.J. Richardson), tom.clarke@uea.ac.uk (T.A. Clarke).

http://dx.doi.org/10.1016/j.febslet.2014.04.013
0014-5793/

mediated by these extracellular cytochromes. We have determined the molecular structure of OmcA to 2.7 Å resolution that, together with the crystal structures of MtrF and UndA allows an evaluation of possible mechanisms of extracellular protein–protein and protein–mineral electron transfer interactions of the *Shewanella* OMMC family.

2. Methods and materials

2.1. Expression and purification of OmcA

The *OmcA*-encoding genes were amplified from *S. oneidensis MR-1* and cloned into a pBAD202 (*Invitrogen)* plasmid. The OmcA protein was solubilized by replacing the N-terminal 25 amino acids with the *S. oneidensis* MR-1 MtrB N-terminus (MKFKLNLITLALLANTGLAVAADG) and adding a C-terminal V5-epitope/6xhis tag (KGELKLEGKPIPNPLLGLDSTRTGHHHHHH) to give pLS147. *S. oneidensis* MR-1 strain LS330 containing pLS147, was grown aerobically at 30 °C in Terrific Broth (TB) media containing 30 μg ml^{-1} kanamycin. Expression was induced by addition of 1 mM L-arabinose at the mid-log phase of growth. Cells were grown overnight and removed from the media by centrifugation. The clarified media was concentrated to ~400 ml using a stirred Amicon pressure cell before dialysis into buffer containing 20 mM HEPES pH 7.8. The dialysed media/protein was centrifuged at 15000×*g* for 15 min to remove any precipitate before loading onto a 200 ml DEAE column pre-equilibrated with 20 mM HEPES pH 7.8. The protein was eluted with a gradient of 0–500 mM NaCl. Fractions were analyzed by SDS–PAGE staining with Coomassie. Fractions containing OmcA were pooled and dialysed into 20 mM HEPES pH 7.6 + 50 mM NaCl before being concentrated to 15 mg ml^{-1} using a centrifugal concentrator.

2.2. OmcA crystalization and data collection

Crystals of OmcA were obtained from a sitting-drop vapor diffusion setup with 0.1 M BIS-TRIS propane pH 8.5, 0.1 M $MgCl_2$ and 15% PEG 20000 as the reservoir solution. Crystals formed in both 1:1 and 2:1 (reservoir:protein) drops with a total drop volume of 0.6 μl. Crystals were cryo-protected by transferring to a solution of 0.1 M BIS-TRIS propane pH 8.5, 0.1 M $MgCl_2$, 15% PEG 20000 and 20% DMSO before being vitrified by plunging into liquid nitrogen. Data were collected on OmcA crystals in a stream of gaseous nitrogen at 100 K on beamline I24 at the Diamond Light Source (UK). OmcA crystals were determined to be of space group $P2_1$ with typical cell dimensions of a = 92.70, b = 245.64, c = 135.51 Å and a β-angle of 97.79°. In order to exploit the ten irons of OmcA data was collected at an X-ray wavelength of 1.72 Å, the theoretical position of the high energy Fe-absorption edge. This yielded a SAD (single-wavelength anomalous dispersion) dataset at a final resolution of 3.5 Å. Further datasets from single crystals were collected to a resolution of 2.7 Å using an X-ray wavelength of 0.97 Å.

2.3. OmcA structure determination and refinement

OmcA datasets were processed using XIA2, or MOSFLM and SCALA as part of the CCP4 package [17–20]. The SAD dataset of OmcA was analyzed using SHELX [21]. After processing using SHELXC and SHELXD a total of 40 iron atoms were identified in the asymmetric unit. Subsequent phasing was performed at a final resolution of 3.5 Å using SHELXE. Electron density maps calculated using these phases were sufficiently interpretable to manually place forty hemes corresponding to 4 OmcA molecules in the asymmetric unit. Model building was carried out using COOT [22] and Buccaneer. The initial model was then used as a search model in molecular replacement run using PHASER [23] to phase the 2.7 Å resolution dataset. The autobuild program Buccaneer was then used to build residues 43–735 followed by alternating rounds of manual building and refinement using PHENIX [24] or REFMAC [25]. The final model was refined to an R_{cryst} (R_{free}) value of 19.3(23.0)% with 4 outliers in the Ramachandran plot. Coordinates have been deposited in the RCSB Protein Data bank under accession code 4LMH.

2.4. Small-angle X-ray scattering

SAXS data collection was performed as previously described [26]. The radii of gyration R_G were derived by the Guinier approximation [27] as implemented PRIMUS from the ATSAS 2.3 software package [28] ($q \cdot Rg < 1.3$). Extrapolation of the scattering intensities to zero angle was performed to correct for concentration effects. Electron pair distance distribution functions, $P(r)$, were obtained by indirect Fourier transformation of intensities using the program GNOM [29]. The maximum intraparticle distance, D_{max} was determined by iterative fitting over a series of D_{max} values spaced by 0.5 Å, to maximize the total estimate as defined in GNOM. The program CRYSOL was used to calculate scattering profiles from crystal structure coordinates of OmcA and the discrepancy (c^2) between experimental and calculated scattering profiles [30].

3. Results and discussion

3.1. X-ray crystal and solution structure of OmcA

The X-ray crystal structure of the *S. oneidensis* MR-1 OmcA was solved by experimental phasing and refined to 2.7 Å resolution (Fig. 1A, Table 1). OmcA is folded into four distinct domains. N-terminal domain I forms a Greek key split β-barrel structure that is connected to domain II, which contains several short α-helices that serve as a scaffold for five *c*-type hemes. A ~20 amino acid α-helix connects domain II to domain III, a second Greek key split β-barrel domain that is connected to domain IV, the C-terminal penta-heme domain. This domain organization is conserved in both the deca-heme MtrF (3.2 Å, PDB ID: 3PMQ) and undeca-heme UndA (1.8 Å, PDB ID: 3UCP) [2,3]. A structure-based alignment of the amino acid sequences of OmcA, MtrF and UndA reveal a number of polypeptide insertions and deletions in each member (Fig. S2). These insertions alter the overall electronegative surface potential of the cytochromes by neutralizing some of the charged propionate groups of the *c*-type hemes and could have a substantial impact on the way that these proteins interact with protein partners or substrates.

OmcA possesses two disulfide bonds, one located within the N-terminal β-barrel domain (domain I) and one within the β-barrel of domain III (Fig. 1A). The cysteines of these disulfides are conserved in the MtrF and UndA sequences (Fig. S2) and the disulfides are structurally conserved in the UndA structure. Only the disulfide of domain III was resolved in MtrF, the putative disulfide bond in domain I has not been resolved in the MtrF structure due to the low resolution of the structure (3.2 Å) and high temperature factor of that domain (160 Å^2).

All the hemes in domains II and IV display *bis*-histidine axial ligand coordination to the heme iron and the histidines that form the distal ligands to the hemes are located within the same domain as the corresponding CXXCH motif. The hemes are arranged in a 'staggered cross' configuration where a 65 Å octa-heme chain formed by hemes 5,4,3,1,6,8,9,10 transects the length of OmcA through domains IV and II. This octa-heme chain is crossed by a 45 Å tetra-heme chain consisting of hemes 2,1,6,7 of OmcA. This tetra-heme chain connect the β-barrel domains I and III. Each heme

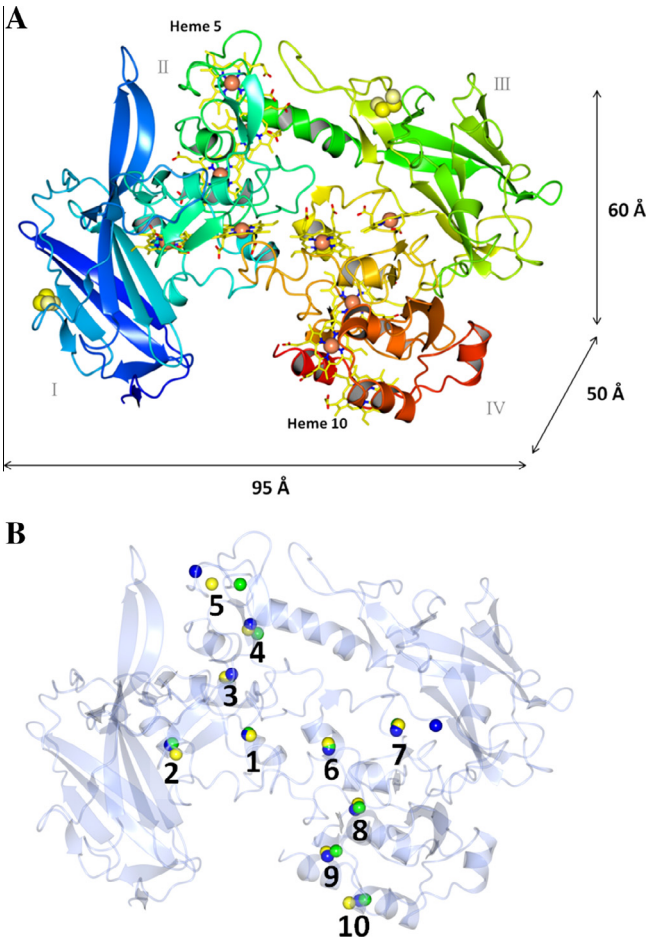

Fig. 1. Crystal structure of OmcA at 2.7 Å resolution (PDB ID: 4LMH). (A) The polypeptide chains are shown in ribbon representation and colored from blue (N-terminus) to red (C-terminus). The domains are indicated by roman numerals. The Fe atoms of the hemes are represented as orange spheres and the porphyrin rings of the hemes are shown as yellow sticks. The crystal structure disulfide bonds are represented as yellow spheres. (B) Superposition of iron atoms from the structures of OmcA (yellow), MtrF (green) and UndA (blue). The polypeptide chain of OmcA is shown as a transparent cartoon while the iron atoms are shown as spheres.

is within 7 Å of its nearest neighbor, ensuring efficient and rapid intra-molecular electron transfer. Superposition of the heme irons of OmcA with the corresponding heme irons of MtrF and UndA reveals that 9 hemes overlay with root mean square deviations (RMSD) of 1.2–2.7 Å. The exception is heme 5, where the RMSD between MtrF and OmcA is 4.3 Å and the RMSD between UndA and OmcA is 9.2 Å. (Fig. 1B; note that UndA contains an extra heme next to heme 7 of OmcA and MtrF).

3.2. Oligomeric state of OmcA

The crystal structure of OmcA reveals four molecules in the asymmetric unit giving a solvent content of 73% (Fig. S3). Superposition of the four OmcA molecules revealed that the overall RMSD between the main-chain atoms of each monomer were less than 0.5 Å, indicating no significant structural differences between the monomers of the asymmetric unit. Analysis of the arrangement of the four OmcA molecules in the asymmetric unit reveals two different orientations where the four monomers can be arranged in two structurally conserved OmcA dimers (Fig. S4). The interfaces of the two dimers have similar surface areas between 488 Å and 580 Å. However, only one dimer orientation allows the two monomers of each potential dimer to interact in such a way as to form an

Table 1
Data collection and refinement statistics (SAD and molecular replacement) for OmcA.

	OmcA-SAD	OmcA-native
Data collection[*]		
Space group	$P\,2_1$	$P\,2_1$
Cell dimensions		
a, *b*, *c* (Å)	92.70, 245.64, 135.51	92.64, 245.38, 135.63
α, β, γ (°)	90.00, 97.79, 90.00	90.00, 97.89, 90.00
Resolution (Å)	91.84–3.5 (3.6–3.5)	58.1–2.7 (2.8–2.7)
R_{sym} or R_{merge} (%)	13.1 (30.3)	9.1 (37.7)
$I/\sigma(I)$	20.5 (9.9)	10.9 (3.1)
Completeness (%)	99.9 (99.9)	98.5 (98.4)
Redundancy	14.1(13.1)	3.0 (2.9)
Refinement		
Resolution (Å)		2.70
No. reflections		161 229
R_{work}/R_{free}		0.19/0.23
No. atoms		
Protein		20 903
Ligand/ion		1728
Water		1748
Avg. *B*-factors		
Protein		38.4
Ligand/ion		33.1
Water		35.0
R.m.s. deviations		
Bond lengths (Å)		0.013
Bond angles (°)		0.889

[*] Values in parentheses are for highest-resolution shell.

interface between heme 5 of each monomer (Fig. 2A). This would give rise to a twenty heme branched wire 169 Å long spanning a distance of 113 Å between the Fe atoms of the terminal hemes (Fig. 2B). This orientation displays non-crystallographic C2 symmetry which is frequently observed for protein homodimers [31], and also positions the N-terminus of each monomer on the same side of the dimer. Under physiological conditions the N-terminal of OmcA is attached to a lipid via an LXXC motif [4], so this dimer could occur on the surface of the cell. A surface loop close to heme 5 contains a tyrosine residue (Tyr^{374}) that is conserved in the OmcA clade and at the crystallographic dimer interface Tyr^{374} from each OmcA monomer comes within H-bonding distance, suggesting that one of the two residues deprotonate to allow a Tyr^{374}–Tyr^{374} H-bond to form (Fig. S5). Structural alignment of the four OmcA molecules in the asymmetric unit to one another reveals no notable domain movements or structural differences beyond the subtle movement of surface exposed side chains as a result of the crystal packing.

To explore the oligomeric state of OmcA in solution, small-angle X-ray scattering (SAXS) data were collected at a range of concentrations for OmcA (2.3–19.2 mg/ml) in both high and low ionic strength buffers (150 mM and 10 mM NaCl, respectively) (Fig. S6). Data collected for OmcA agreed with previously published SAXS data for OmcA [26] indicating a monomer in solution. The experimental SAXS data for OmcA gave a radius of gyration (R_G) of 30.6 ± 0.2 Å and a maximum dimension (D_{max}) of 96 Å consistent with values calculated for a single monomer using crystal structure coordinates (R_G = 30.2 Å, D_{max} = 97 Å). The overall molecular conformation of OmcA in the crystal structure is in excellent agreement (x^2 = 1.630) with the molecular shape of OmcA in solution (Fig. S6C and D). Thus, under the conditions in which OmcA is purified the protein behaves as a monomer in solution suggesting that any protein–protein interactions that govern the dimer assembly observed in the crystal structure are weak. This is reflected by the rather low interaction surface area of ~500 $Å^2$ between the monomers of the icosa-heme wire, which is consistent with the observed solution state.

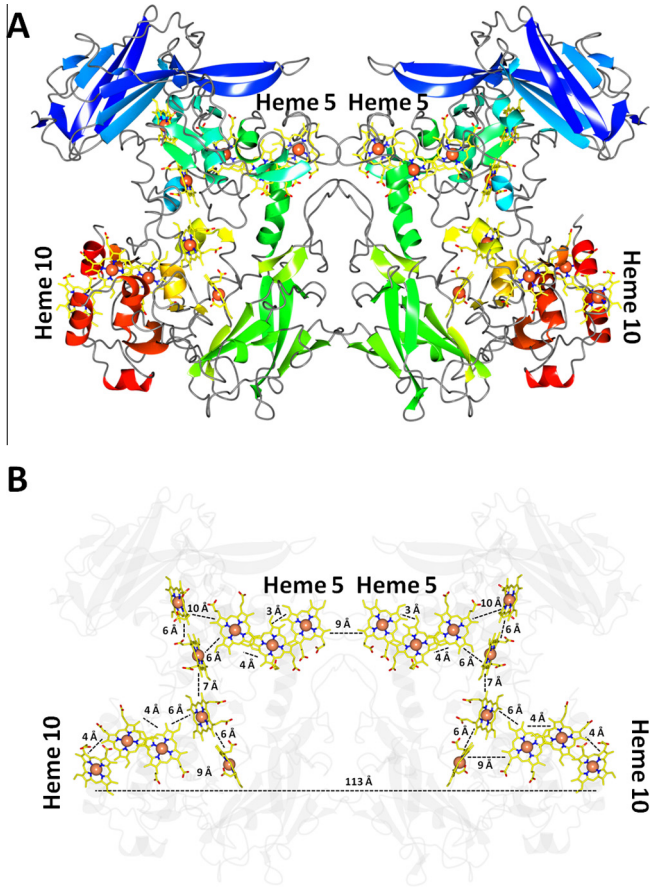

Fig. 2. Dimer assembly and heme arrangement within OmcA. (A) Arrangement of monomers in the potential OmcA dimer found within the crystallographic asymmetric unit. The polypeptide chains of the OmcA molecules are shown in cartoon representations and colored from blue (N-terminus) to red (C-terminus). (B) Heme–heme distances of potential OmcA dimers found within the asymmetric unit. The polypeptide chains are shown as a transparent grey background in cartoon representation. Hemes of both OmcA molecules are shown as yellow cylinders with the Fe atoms shown as orange spheres.

3.3. Hydroxylated surface of OmcA

OmcA has a highly hydroxylated protein surface, contributed to by threonine and serine residues (Fig. 3A). A proposed 'hematite binding motif' that has a conserved sequence of Ser/Thr-Pro-Ser/Thr was identified in the amino acid sequence of OmcA by Lower et al. who utilized phage-display technology to enrich for a number of peptides that were rich in amino acids with polar side chains, notably serine and threonine [32]. Molecular dynamic simulations with the peptide Ser-Pro-Ser indicated that hydrogen bonding occurs between two serines and the hydroxylated hematite surface and that the proline induces a structure-binding motif by limiting the peptide flexibility [32]. From the crystal structures we can identify this motif, Thr-Pro-Ser (OmcA) near the terminal heme-binding domain (hemes 9 & 10) of OmcA (Fig. 3B). The hydroxyl side chains face outwards from the protein surface and are positioned such that the distance from the Fe centers of terminal heme groups to the Cα of the closest residue in the hematite binding motif is ~10 Å.

3.4. Insights into possible mechanisms of inter-protein electron transfer in the OMMCs

Electron exchange between multi-heme cytochromes must take place in the extracellular environment so that electrons can move from cytochromes in the tightly bound cell surface lipopolysaccharide (LPS) to those located in the more loosely bound LPS matrix [33]. As a conduit between cell and mineral surface OmcA is likely to have two sites for electron exchange; the OmcA crystal structure reveals the most likely candidates to be hemes 5 and 10. The heme arrangement at the two electron transfer sites is likely to be more conserved at the active site where mineral binding and reduction are to occur. While the arrangement of hemes at the electron ingress site is likely to be divergent as each OMMC interact with a range of different partners. MtrF and MtrC associate tightly with MtrDE and MtrAB complexes embedded in the outer membrane, while OmcA and UndA are thought to accept electrons from either the MtrCAB or MtrDEF complexes. A 2:1 complex has been reported for OmcA:MtrC in solution [34], and this would be consistent with one OmcA dimer interacting with a single MtrCAB complex. Heme 5 shows the greatest variation in heme position and orientation between the three structures, which suggests this might be the site for electron exchange between different protein partners. The ability of OmcA to form a crystallographic dimer with heme 5 at the interface is also consistent with heme 5 being the site of cytochrome–cytochrome interaction and may form the dimer observed on the surface of the cell. This would leave heme 10, exposed in a patch of hydroxylated residues to serve as the electron egress site to mineral or metal ion.

Acknowledgements

DJR is a Royal Society Wolfson Foundation Merit Award holder. This research was supported by the Biotechnology and Biological

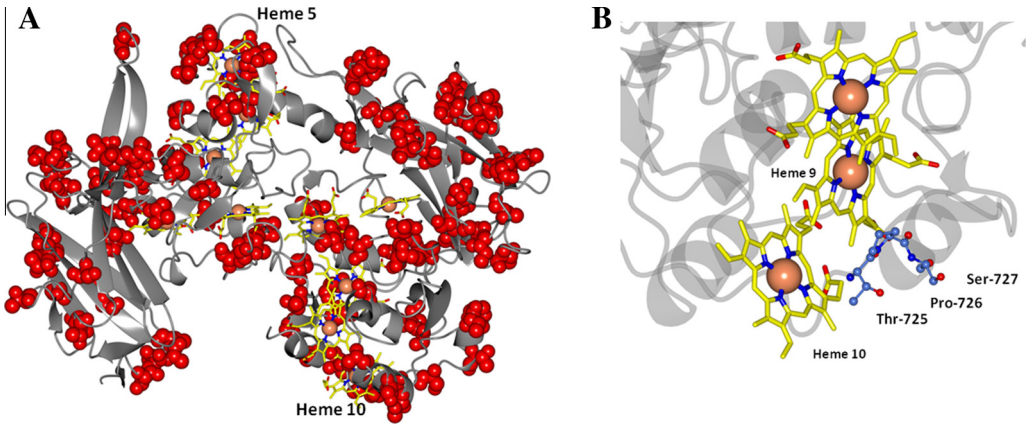

Fig. 3. Hydroxylated surface of OmcA showing motif. (A) Distribution of serine and threonine residues of OmcA. Red spheres indicate the positions of atoms of serine/threonine residues. (B) Residues of the proposed hematite binding motif of OmcA, as identified by Lower et al. [32], shown in ball and stick representation.

Sciences Research Council (BB/K00929X/1 and BB/H007288/1) and sponsored by the Subsurface Biogeochemical Research program (SBR)/Office of Biological and Environmental Research (BER), U.S. Department of Energy (DOE), and is a contribution of the Pacific Northwest National Laboratory (PNNL) Scientific Focus Area and the Mercury Scientific Focus Area at Oak Ridge National Laboratory (ORNL). The PNNL and ORNL are operated for the DOE by Battelle under contracts DE-AC05-76RLO1830 and DE-AC05-00OR22725

Appendix A. Supplementary data

Supplementary data associated with this article can be found, in the online version, at http://dx.doi.org/10.1016/j.febslet.2014.04.013.

References

[1] Richardson, D.J. et al. (2012) The porin-cytochrome model for microbe-to-mineral electron transfer. Mol. Microbiol. 85, 201–212.
[2] Clarke, T.A. et al. (2011) Structure of a bacterial cell surface decaheme electron conduit. Proc. Natl. Acad. Sci. U.S.A. 108, 9384–9389.
[3] Edwards, M.J., Hall, A., Shi, L., Fredrickson, J.K., Zachara, J.M., Butt, J.N., Richardson, D.J. and Clarke, T.A. (2012) The crystal structure of the extracellular 11-heme cytochrome UndA reveals a conserved 10-heme motif and defined binding site for soluble iron chelates. Structure 20, 1275–1284.
[4] Mitchell, A.C., Peterson, L., Reardon, C.L., Reed, S.B., Culley, D.E., Romine, M.R. and Geesey, G.G. (2012) Role of outer membrane c-type cytochromes MtrC and OmcA in *Shewanella oneidensis* MR-1 cell production, accumulation, and detachment during respiration on hematite. Geobiology 10, 355–370.
[5] Belchik, S.M. et al. (2011) Extracellular reduction of hexavalent chromium by cytochromes MtrC and OmcA of *Shewanella oneidensis* MR-1. Appl. Environ. Microbiol. 77, 4035–4041.
[6] Coursolle, D., Baron, D.B., Bond, D.R. and Gralnick, J.A. (2010) The Mtr respiratory pathway is essential for reducing flavins and electrodes in *Shewanella oneidensis*. J. Bacteriol. 192, 467–474.
[7] Ross, D.E., Brantley, S.L. and Tien, M. (2009) Kinetic characterization of OmcA and MtrC, terminal reductases involved in respiratory electron transfer for dissimilatory iron reduction in *Shewanella oneidensis* MR-1. Appl. Environ. Microbiol. 75, 5218–5226.
[8] Shi, L. et al. (2008) Direct involvement of type II secretion system in extracellular translocation of *Shewanella oneidensis* outer membrane cytochromes MtrC and OmcA. J. Bacteriol. 190, 5512–5516.
[9] Cheung, A.C.M., Bretschger, O., Mansfeld, F. and Nealson, K.H. FUEL 127-Performance of different strains of the senus Shewanella in a microbial fuel cell. Abstracts of Papers of the American Chemical Society 234 (2007).
[10] Firer-Sherwood, M., Pulcu, G.S. and Elliott, S.J. (2008) Electrochemical interrogations of the Mtr cytochromes from *Shewanella*: opening a potential window. J. Biol. Inorg. Chem. 13, 849–854.
[11] Hartshorne, R.S. et al. (2007) Characterization of *Shewanella oneidensis* MtrC: a cell-surface decaheme cytochrome involved in respiratory electron transport to extracellular electron acceptors. J. Biol. Inorg. Chem. 12, 1083–1094.
[12] Lower, B.H., Shi, L., Yongsunthon, R., Droubay, T.C., McCready, D.E. and Lower, S.K. (2007) Specific bonds between an iron oxide surface and outer membrane cytochromes MtrC and OmcA from *Shewanella oneidensis* MR-1. J. Bacteriol. 189, 4944–4952.
[13] Ross, D.E., Ruebush, S.S., Brantley, S.L., Hartshorne, R.S., Clarke, T.A., Richardson, D.J. and Tien, M. (2007) Characterization of protein–protein interactions involved in iron reduction by *Shewanella oneidensis* MR-1. Appl. Environ. Microbiol. 73, 5797–5808.
[14] Xiong, Y. et al. (2006) High-affinity binding and direct electron transfer to solid metals by the *Shewanella oneidensis* MR-1 outer membrane c-type cytochrome OmcA. J. Am. Chem. Soc. 128, 13978–13979.
[15] Eggleston, C.M., Vörös, J., Shi, L., Lower, B.H., Droubay, T.C. and Colberg, P.J.S. (2008) Binding and direct electrochemistry of OmcA, an outer-membrane cytochrome from an iron reducing bacterium, with oxide electrodes: a candidate biofuel cell system. Inorg. Chim. Acta 361, 769–777.
[16] Johs, A., Shi, L., Droubay, T., Ankner, J.F. and Liang, L. (2010) Characterization of the decaheme *c*-type cytochrome OmcA in solution and on hematite surfaces by small angle X-ray scattering and neutron reflectometry. Biophys. J. 98, 3035–3043.
[17] Bailey, S. (1994) The CCP4 suite – programs for protein crystallography. Acta Crystallogr. D Biol. Crystallogr. 50, 760–763.
[18] Leslie, A.G.W. (1999) Integration of macromolecular diffraction data. Acta Crystallogr. D Biol. Crystallogr. 55, 1696–1702.
[19] Evans, P. (2006) Scaling and assessment of data quality. Acta Crystallogr. D Biol. Crystallogr. 62, 72–82.
[20] Winter, G. (2010) Xia2: an expert system for macromolecular crystallography data reduction. J. Appl. Crystallogr. 43, 186–190.
[21] Sheldrick, G.M. (2008) A short history of SHELX. Acta Crystallogr. A 64, 112–122.
[22] Emsley, P. and Cowtan, K. (2004) Coot: model-building tools for molecular graphics. Acta Crystallogr. D Biol. Crystallogr. 60, 2126–2132.
[23] McCoy, A.J., Grosse-Kunstleve, R.W., Adams, P.D., Winn, M.D., Storoni, L.C. and Read, R.J. (2007) Phaser crystallographic software. J. Appl. Crystallogr. 40, 658–674.
[24] Adams, P.D. et al. (2010) PHENIX: a comprehensive Python-based system for macromolecular structure solution. Acta Crystallogr. D Biol. Crystallogr. 66, 213–221.
[25] Murshudov, G.N. et al. (2011) REFMAC5 for the refinement of macromolecular crystal structures. Acta Crystallogr. D Biol. Crystallogr. 67, 355–367.
[26] Johs, A., Shi, L., Droubay, T., Ankner, J.F. and Liang, L. (2010) Characterization of the decaheme c-type cytochrome OmcA in solution and on hematite surfaces by small angle X-ray scattering and neutron reflectometry. Biophys. J. 98, 3035–3043.
[27] Guinier, A. and Fournet, G. (1955) Small Angle Scattering of X-rays, Wiley, New York.
[28] Konarev, P.V., Petoukhov, M.V., Volkov, V.V. and Svergun, D.I. (2006) ATSAS 2.1, a program package for small-angle scattering data analysis. J. Appl. Crystallogr. 39, 277–286.
[29] Svergun, D.I. (1992) Determination of the regularization parameter in indirect-transform methods using perceptual criteria. J. Appl. Crystallogr. 25, 495–503.
[30] Svergun, D., Barberato, C. and Koch, M.H.J. (1995) CRYSOL – a program to evaluate X-ray solution scattering of biological macromolecules from atomic coordinates. J. Appl. Crystallogr. 28, 768–773.
[31] Goodsell, D.S. and Olson, A.J. (2000) Structural symmetry and protein function. Annu. Rev. Biophys. Biomol. Struct. 29, 105–153.
[32] Lower, B.H., Lins, R.D., Oestreicher, Z., Straatsma, T.P., Hochella Jr., M.F., Shi, L. and Lower, S.K. (2008) In vitro evolution of a peptide with a hematite binding motif that may constitute a natural metal-oxide binding archetype. Environ. Sci. Technol. 42, 3821–3827.
[33] Cao, B. et al. (2011) Extracellular polymeric substances from *Shewanella* sp. HRCR-1 biofilms: characterization by infrared spectroscopy and proteomics. Environ. Microbiol. 13, 1018–1031.
[34] Shi, L. et al. (2006) Isolation of a high-affinity functional protein complex between OmcA and MtrC: two outer membrane decaheme *c*-type cytochromes of *Shewanella oneidensis* MR-1. J. Bacteriol. 188, 4705–4714.